

# REDUCED ORDER DISTRIBUTED PARTICLE FILTER FOR ELECTRIC POWER GRIDS

Amir Asif, Arash Mohammadi, and Shivam Saxena

Department of Electrical Engineering and Computer Science  
York University, Toronto, ON, Canada M3J 1P3. Email: {marash, asif}@cse.yorku.ca

## ABSTRACT

The paper develops a fusion-based, reduced order, distributed implementation of the unscented particle filter (FR/DUPF) for state estimation in complex nonlinear electric power grids (EPG). Based on partitioning the overall EPG system into  $n_{\text{sub}}$  localized but dynamically coupled subsystems, the near-optimal FR/DUPF provides a computational saving of up to a factor of  $n_{\text{sub}}$  over the centralized particle filter. In our Monte Carlo simulations of the IEEE 14-bus test system, the FR/DUPF state estimates are close to the actual values and virtually indistinguishable from the centralized particle filter.

**Index Terms**— Distributed estimation, Large scale dynamical systems, Nonlinear estimation, Particle filtering, Smart power grids.

## 1. INTRODUCTION

The paper derives *nonlinear* data fusion algorithms for large scale, geographically distributed dynamical systems observed sparsely by a network of spatially dispersed nodes with the objective of estimating the states of the overall system. Of particular interest is distributed state estimation [1]-[3] in electric power grids (EPG) [4]-[17], where state estimates are used to monitor grid status, optimize power flows, enable energy management, and perform reliability assessment.

While for linear systems, the Kalman filter is typically the ideal choice, nonlinear state-space models do not permit analytic solutions. As a sequential analogue of the extended/unscented Kalman filter (EKF/UKF), the particle filter [18, 19] is increasingly being used to solve such nonlinear estimation problems in an online, recursive manner with the added advantage that the filter approaches the optimal Bayesian estimator provided sufficient samples of the posterior distribution are available. Recent state estimation approaches [6]-[9] in EPGs consider a centralized estimation architecture where all measurements are available at a central location, referred to as the fusion centre. These centralized approaches are computationally intensive and require a large number of information transfers from the nodes constituting the EPG to its fusion centre adding considerable latency to the estimation mechanism. In this paper, we propose a different framework based on a fusion-based reduced order, distributed implementation of the unscented particle filter (FR/DUPF) that partitions the overall system into  $n_{\text{sub}}$  localized but analytically coupled subsystems. Recall that coupled subsystems typically share states with their immediate neighbors. Unlike the existing reduced-order state estimation approaches [20, 21] that completely decouple subsystems from each other, the state dynamics of the subsystems in the FR/DUPF overlap. The system remains coupled through interactions between the local subsystems. The FR/DUPF ensures consistency between its localized marginal filtering distributions by introducing state and observation fusion steps between the neighboring subsystems. Since each subsystem estimates a subset of the overall state vector without the need of a centralized fusion centre, the FR/DUPF

provides a computational saving of up to a factor of  $n_{\text{sub}}$  over its centralized counterpart thus overcoming the dimensionality impediment [33, 34] associated with the EPGs. Based on the IEEE 14-bus test system, our Monte Carlo simulations show that the proposed FR/DUPF is near-optimal and follows the centralized filter closely.

The paper is organized as follows. Section 2 presents the EPG state-space model as well as its reduced-order representation used in Section 3 to derive the FR/DUPF. Based on the IEEE 14 bus test system, Section 4 runs Monte Carlo simulations to quantify the performance of the FR/DUPF. Finally, Section 5 concludes the paper.

## 2. NON-LINEAR STATE-SPACE EPG MODEL

An EPG is a complex electrical network that supplies electricity produced by power generators (referred to as the generator nodes) to geographically distributed subscribers (referred to as load nodes) through transmission lines and transformers. Without loss of generality, we assume that nodes 1 to  $n_G$  are the generator nodes, while nodes  $n_G + 1$  to  $N$  are the load nodes. The state vector is given by

$$\mathbf{x}(t) = [\mathbf{x}_G^T(t), \mathbf{x}_L^T(t)]^T, \quad (1)$$

where the  $(3n_G - 1)$  states corresponding to the generator nodes are

$$\mathbf{x}_G(t) = [V_1(t), \omega_1(t), V_2(t), \theta_2(t), \omega_2(t) \dots V_{n_G}(t), \theta_{n_G}(t), \omega_{n_G}(t)]^T,$$

and the  $2(N - n_G)$  states corresponding to the load nodes are

$$\mathbf{x}_L(t) = [V_{n_G+1}(t), \theta_{n_G+1}(t), \dots, V_N(t), \theta_N(t)]^T.$$

While voltage  $V_i$  and its phase  $\theta_i$  are state variables common at both generator and load nodes, the angular velocity  $\omega_i$  associated with the rotor of generator  $i$  supplements generator's state vector  $\mathbf{x}_G$ , for  $(1 \leq i \leq n_G)$ . The phase  $\theta_1$  at node 1 is assumed 0 with other phases measured with respect to this reference phase. At generator node  $i$ , the voltage, phase, and angular velocity [15, 17] are given by

$$\begin{aligned} \frac{dV_i(t)}{dt} &= (1/T_{do_i})E_{f_i} - 1/T_{do_i}V_i + 1/T_{do_i}(X_{d_i} - X'_{d_i}) \\ &\times \sum \{V_j(G_{ij} \sin(\theta_i - \theta_j) - B_{ij} \cos(\theta_{ij}))\} + \xi_{1,i} \end{aligned} \quad (2)$$

$$\frac{d\theta_i(t)}{dt} = \omega_i(t) + \xi_{2,i} \quad (3)$$

$$\begin{aligned} \frac{d\omega_i(t)}{dt} &= -D_i/J_i \times \omega_i + 1/J_i \times P_{m_i} \\ &- 1/J \sum V_j V_i \{B_{ij} \sin(\theta_{ij}) - G_{ij} \cos(\theta_{ij})\} + \xi_{3,i}, \end{aligned} \quad (4)$$

with the limits of the summations given by  $(1 \leq j \leq N)$ . To save on space, variable  $t$  used to express the dependency of the states on time is dropped in the expressions above and hereafter. The phase difference  $\theta_{ij}(t)$  equals  $\theta_i(t) - \theta_j(t)$ ; admittance  $G_{ij} + jB_{ij}$  is entry  $(i, j)$

of the admittance matrix  $\mathbf{Y}$  representing the connectivity between EPG nodes  $i$  and  $j$ , and;  $\{J_i, D_i\}$  the rotor inertia and damping factor of generator  $i$ . Associated with generator  $i$  are its mechanical input power  $P_{m_i}$  and electromagnetic field  $E_f$  used for excitation. Term  $(X_{d_i} - X_{d'_i})$  is the difference between the direct and transient axis' reactances;  $T_{do_i}$  the direct-axis transient time constant, and  $\xi_i(t) = [\xi_{1,i}(t), \xi_{2,i}(t), \xi_{3,i}(t)]^T$  the process noise vector for generator  $i$ . Likewise, the state model [16] for load node  $i$  is given by

$$\frac{dV_i(t)}{dt} = -\frac{1}{\kappa_{Q_i}} \left\{ \sum V_i V_j (G_{ij} \sin(\theta_{ij}) - B_{ij} \cos(\theta_{ij})) + Q_{si}(V_i) \right\} + \frac{\eta_i h_i}{\kappa_{Q_i}} + \xi_{1,i}, \quad (5)$$

$$\frac{d\theta_i(t)}{dt} = -\frac{1}{\kappa_{P_i}} \left\{ \sum V_i V_j (G_{ij} \cos(\theta_{ij}) - B_{ij} \sin(\theta_{ij})) + P_{si}(V_i) \right\} + 1/\kappa_{P_i} h_i + \xi_{2,i}, \quad (6)$$

where  $\{P_{si}, Q_{si}\}$  represents the static real and reactive load demand at node  $i$  as a function of  $V_i$ , constants  $\{\kappa_{P_i}, \kappa_{Q_i}\}$  relate the dynamic load components to the rate of change in the local frequency and voltage at load node  $i$ , and variable  $h_i$  is the real power load disconnected during load shedding and considered as a control input. Parameter  $\eta_i$  denotes the power factor of load node  $i$ . Eqs. (2)-(6) represent the EPG state model, which collectively are represented as

$$\frac{d\mathbf{x}(t)}{dt} = \mathbf{f}_1(\mathbf{x}(t)) + \boldsymbol{\xi}(t) \quad (7)$$

**Observation Model:** depends on active and reactive line power flows

$$P_{ij}(t) = V_i^2(G_{ij}) - V_i V_j (G_{ij} \cos \theta_{ij} + B_{ij} \sin \theta_{ij}) \quad (8)$$

$$Q_{ij}(t) = -V_i^2(B_{ij}) - V_i V_j (G_{ij} \sin \theta_{ij} + B_{ij} \cos \theta_{ij}), \quad (9)$$

and active and reactive bus power injections  $\{P_{ii}, Q_{ii}\}$  given by

$$P_{ii}(t) = V_i \sum_{j \in \mathbb{N}_i} V_j (G_{ij} \cos \theta_{ij} + B_{ij} \sin \theta_{ij}) \quad (10)$$

$$Q_{ii}(t) = V_i \sum_{j \in \mathbb{N}_i} V_j (G_{ij} \sin \theta_{ij} + B_{ij} \cos \theta_{ij}), \quad (11)$$

where  $\mathbb{N}_i$  is the subset of buses connected to bus  $i$  as specified in the admittance matrix  $\mathbf{Y}$ . Collecting (8)-(11), the observation model is

$$\mathbf{z}(t) = \mathbf{g}(\mathbf{x}(t)) + \boldsymbol{\zeta}(t), \quad (12)$$

where  $\boldsymbol{\zeta}(t)$  denotes observation uncertainties. Discretizing (7) and (12) using a finite-difference scheme leads to the state-space model

$$\text{State Model: } \mathbf{x}(k) = \mathbf{f}(\mathbf{x}(k-1)) + \boldsymbol{\xi}(k), \quad (13)$$

Observation Model:

$$\underbrace{\begin{bmatrix} Z_1(k) \\ \vdots \\ Z_{n_z}(k) \end{bmatrix}}_{\mathbf{z}(k)} = \underbrace{\begin{bmatrix} \mathbf{g}_1(\mathbf{x}(k)) \\ \vdots \\ \mathbf{g}_{n_z}(\mathbf{x}(k)) \end{bmatrix}}_{\mathbf{g}(\mathbf{x}(k))} + \underbrace{\begin{bmatrix} \zeta_1(k) \\ \vdots \\ \zeta_{n_z}(k) \end{bmatrix}}_{\boldsymbol{\zeta}(k)}, \quad (14)$$

where  $\mathbf{f}(\mathbf{x}(k)) = \mathbf{x}(k) + \Delta T \times \mathbf{f}_1(\mathbf{x}(k))$  used to derive (13) from (7),  $n_z$  is the number of observation nodes, and  $\Delta T$  is the time step.

### 2.1. Distributed Reduced-Order Configuration

In large-scale EPGs, measurements  $Z_m(k)$ , ( $1 \leq m \leq n_z$ ), are localized and depend on a subset of state variables. In the proposed FR/DUPF, the reduced-order state-space model at node  $l$  is obtained

by spatially decomposing the overall system (Eq. (13)) into  $n_{\text{sub}}$  subsystems based on the observable states  $\mathbf{x}^{(l)}(k)$  at that node as

$$S_l : \mathbf{x}^{(l)}(k) = \mathbf{f}^{(l)}(\mathbf{x}^{(l)}(k-1), \mathbf{d}^{(l)}(k-1)) + \boldsymbol{\xi}^{(l)}(k). \quad (15)$$

With the above partitioning, Eq. (15) may contain states that are not directly observed by the subsystem but are part of the global state model. The coupling force vector  $\mathbf{d}^{(l)}(k)$  includes such states. Further, a local observation vector  $\mathbf{z}^{(l)}(k)$  is attributed to subsystem  $S_l$ , which is a collection of measurements made at that subsystem. i.e.,

$$S_l : \mathbf{z}^{(l)}(k) = \mathbf{g}^{(l)}(\mathbf{x}^{(l)}(k)) + \boldsymbol{\zeta}^{(l)}(k), \text{ for } (1 \leq l \leq n_{\text{sub}}) \quad (16)$$

The local state vectors  $\mathbf{x}^{(l)}(k)$  in (15)-(16) may have shared states between adjacent nodes, i.e.,  $|\mathbf{x}^{(l)}(k) \cap \mathbf{x}^{(j)}(k)| \geq 0$ , where  $|\cdot|$  is cardinality of a set. Let  $n_{x^{(l)}}$  denote the number of states in the local state vector  $\mathbf{x}^{(l)}(k)$ . The relationship between the local state vector  $\mathbf{x}^{(l)}(k)$  and global vector  $\mathbf{x}(k)$  can then be expressed as

$$\mathbf{x}^{(l)}(k) = \mathbf{T}^{(l)}(k) \mathbf{x}(k), \quad (17)$$

with  $\mathbf{T}^{(l)}(k)$  denoting the  $(n_{x^{(l)}} \times n_x)$  nodal transformation matrix [32]. The local state estimate at node  $l$  has the same relation to the global state estimate, i.e.,  $\hat{\mathbf{x}}^{(l)}(k) = \mathbf{T}^{(l)}(k) \hat{\mathbf{x}}(k)$ . The local process functions also use a similar nodal transformation

$$\mathbf{f}^{(l)}(\mathbf{x}^{(l)}(k), \mathbf{d}^{(l)}(k)) = \mathbf{T}^{(l)}(k) \mathbf{f}(\mathbf{x}(k)). \quad (18)$$

Further, the relationship between the global covariance  $\hat{\mathbf{P}}(k)$  for  $\mathbf{x}(k)$  and local covariance matrix  $\hat{\mathbf{P}}^{(l)}(k)$  for  $\hat{\mathbf{x}}^{(l)}(k)$  is given by

$$\hat{\mathbf{P}}^{(l)}(k) = \mathbf{T}^{(l)}(k) \hat{\mathbf{P}}(k) [\mathbf{T}^{(l)}(k)]^T. \quad (19)$$

To arrange node  $l$ 's information  $\hat{\mathbf{P}}^{(l)}(k)$  in the global state-space, we use the covariance transformation

$$\hat{\mathbf{P}}_G^{(l)}(k) = [\mathbf{T}^{(l)}(k)]^+ \hat{\mathbf{P}}^{(l)}(k) [\mathbf{T}^{(l)}(k)]^{+T}. \quad (20)$$

where  $[\mathbf{T}^{(l)}(k)]^+ = \mathbf{T}^{(l)T}(k) [\mathbf{T}^{(l)}(k) \mathbf{T}^{(l)T}(k)]^{-1}$  refers to the Moore-Penrose generalized inverse. Similar expressions for deriving the covariance of the shared states and global covariance from local covariance matrices are derived in [39]. In the next section, two neighborhood sets are used. Set  $\mathcal{G}^{(l)}$  constitute the nodes in the neighborhood of node  $l$  with which it communicates. In comparison, Set  $\mathcal{G}_n$  for state  $X_n$  contains all nodes where  $X_n$  is included as a state in the localized state vector. Finally, we note that partitioning used in (15)-(16) is achieved by implementing a subsystem at each observation node. Thus, the number of subsystems equals the number of observation nodes. To limit the number of subsystems, a combination of nodes may instead be coupled to form a subsystem.

### 3. REDUCED ORDER FR/DUPF

In the FR/DUPF, each subsystem  $S_l$  runs its local unscented particle filter (UPF) based on the localized models, (15)-(16). Thus, local particles  $\mathbb{X}_i^{(l)}(k)$  and weights  $W_i^{(l)}(k)$ , ( $1 \leq i \leq N_s^{(l)}$ ), are associated with each subsystem  $S_l$ . Notation  $N_s^{(l)}$  denotes the total number of vector particles  $\mathbb{X}_i^{(l)}(k)$  used to represent state  $\mathbf{x}^{(l)}(k)$  in the particle filter. In addition, the particle update at each subsystem requires forcing terms  $\mathbf{d}^{(l)}(k)$  that are obtained from the neighboring subsystems. Next, the FR/DUPF is explained in terms of four stages: Local particles update via UPF; Observation fusion to update weights associated with the local particles; State fusion to form consistent estimates for states common between nodes; and Computation of local forcing terms. Iteration  $k$  of the FR/DUPF is explained below.

**Local Particles Update via UPF:** The UPF couples the particle filter with the unscented Kalman filter (UKF). The optimal proposal distribution function is, therefore, approximated as a Gaussian whose statistics (mean and covariance matrix) are computed using the UKF. The UPF implemented at each subsystem  $S_l$  computes the marginal posterior density of the local state variables based on these statistics. Below, we illustrate the working of the FR/DUPF for iteration  $k$ . In our explanation, the FR/DUPF is assumed to be in steady state prior to iteration  $k$ , i.e., all nodes have computed the state estimates  $\hat{\mathbf{x}}^{(l)}(k-1)$  and covariance  $\hat{\mathbf{P}}^{(l)}(k-1)$  from their individual particle sets. Local measurement  $\mathbf{z}^{(l)}(k)$  is available at subsystem  $S_l$ , which estimates the local posterior as follows.

*Step 1.* Subsystem  $S_l$  generates the set of deterministic samples (sigma points)  $\mathcal{S} = \{\mathcal{W}_i^{(l)}, \chi_i^{(l)}(k-1)\}$ , for  $(0 \leq i \leq 2n_{x(l)})$ , as

$$\chi_i^{(l)}(k-1) = \hat{\mathbf{x}}^{(l)}(k-1) \pm \left\{ \sqrt{(n_{x(l)} + \kappa) \hat{\mathbf{P}}^{(l)}(k-1)} \right\}_i. \quad (21)$$

The square root term corresponds to column  $i$  of the square root of the enclosed matrix. The associated weights  $\mathcal{W}_i^{(l)} = 0.5/(n_{x(l)} + \kappa)$ , where  $\kappa$  is a scaling parameter set between 0 and 1. The initial conditions are  $\chi_0^{(l)}(k) = \hat{\mathbf{x}}^{(l)}(k)$  and  $\mathcal{W}_0^{(l)} = \kappa/(n_{x(l)} + \kappa)$ .

*Step 2.* The Sigma points computed in Step 1 are propagated through the local state model (15) to generate the predicted sigma points

$$\chi_i^{(l)}(k|k-1) = \mathbf{f}^{(l)}(\chi_i^{(l)}(k-1), \mathbf{d}^{(l)}(k-1)), \quad (0 \leq l \leq 2n_{x(l)}). \quad (22)$$

*Step 3.* The predicted sigma points  $\chi_i^{(l)}(k|k-1)$  are now propagated through the local observation model (16) to generate the predicted observation sigma points

$$\mathcal{Z}_i^{(l)}(k|k-1) = \mathbf{g}(\chi_i^{(l)}(k|k-1)), \quad \text{for } (0 \leq l \leq 2n_{x(l)}). \quad (23)$$

*Step 4.* The predicted state estimate, its error covariance matrix, and the predicted observation estimate are then computed as follows

$$\mathbf{x}_{\text{UKF}}^{(l)}(k|k-1) = \sum \mathcal{W}_i^{(l)} \chi_i^{(l)}(k|k-1), \quad (24)$$

$$\mathbf{P}_{\text{UKF}}^{(l)}(k|k-1) = \sum \mathcal{W}_i^{(l)} \left( \chi_i^{(l)}(k|k-1) - \mathbf{x}_{\text{UKF}}^{(l)}(k|k-1) \right) \times \left( \chi_i^{(l)}(k|k-1) - \mathbf{x}_{\text{UKF}}^{(l)}(k|k-1) \right)^T, \quad (25)$$

$$\mathbf{z}_{\text{AUX}}^{(l)}(k|k-1) = \sum \mathcal{W}_i^{(l)} \mathcal{Z}_i^{(l)}(k|k-1). \quad (26)$$

The summations (and the ones below) are indexed  $(0 \leq i \leq 2n_{x(l)})$ .

*Step 5.* The covariance  $\mathbf{P}_{zz}(k|k-1)$  and cross-covariance  $\mathbf{P}_{xz}(k|k-1)$  between predicted states and observations are computed as

$$\mathbf{P}_{zz}^{(l)}(k|k-1) = \sum \mathcal{W}_i^{(l)} \left( \mathcal{Z}_i^{(l)}(k|k-1) - \mathbf{z}^{(l)}(k|k-1) \right) \times \left( \mathcal{Z}_i^{(l)}(k|k-1) - \mathbf{z}^{(l)}(k|k-1) \right)^T, \quad (27)$$

$$\mathbf{P}_{xz}^{(l)}(k|k-1) = \sum \mathcal{W}_i^{(l)} \left( \chi_i^{(l)}(k|k-1) - \mathbf{x}_{\text{UKF}}^{(l)}(k|k-1) \right) \times \left( \mathcal{Z}_i^{(l)}(k|k-1) - \mathbf{z}_{\text{UKF}}^{(l)}(k|k-1) \right)^T. \quad (28)$$

*Step 6.* The statistics for the proposal distribution is estimated as

$$\mathbf{x}_{\text{UKF}}^{(l)}(k) = \mathbf{x}_{\text{UKF}}^{(l)}(k|k-1) + \mathcal{K}^{(l)}(k) \left( \mathbf{z}^{(l)}(k) - \mathbf{z}_{\text{UKF}}^{(l)}(k|k-1) \right) \quad (29)$$

$$\mathbf{P}_{\text{UKF}}^{(l)}(k) = \mathbf{P}_{\text{UKF}}^{(l)}(k|k-1) - \mathcal{K}^{(l)}(k) \mathbf{P}_{zz}^{(l)}(k|k-1) \mathcal{K}^{(l)T}(k) \quad (30)$$

where the Kalman gain  $\mathcal{K}^{(l)}(k) = \mathbf{P}_{xz}^{(l)}(k|k-1) \mathbf{P}_{zz}^{(l)}(k|k-1)^{-1}$ . The proposal distribution is Normal, given by  $\mathcal{N}(\mathbf{x}_{\text{UKF}}^{(l)}(k), \mathbf{P}_{\text{UKF}}^{(l)}(k))$ .

*Step 7.* Each subsystem generates  $N_s^{(l)}$  particles from its local proposal distribution derived in Step 6 completing the local UPF stage.

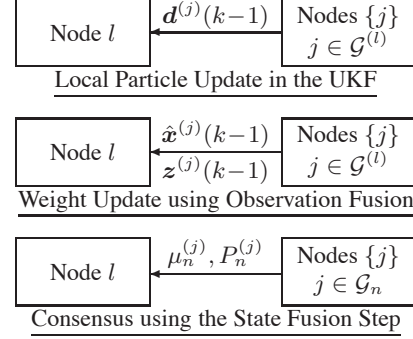


**Fig. 1.** Data transfers for different stages of the FR/DUPF at iteration  $k$ .

**Weight Update using Observation Fusion:** Having updated the local state particles at each subsystem, the next stage computes their weights. The FR/DUPF approximates the weight update equation as a function of two terms: one depends on local state estimates and other on state estimates in the immediate neighborhood as follows

$$W_i^{(l)}(k) \propto W_i^{(l)}(k-1) P\left(\mathbf{z}(k) | \mathbb{X}_i^{(l)}(k), \hat{\mathbf{x}}^{(\neq l)}(k|k-1)\right) \times \frac{P\left(\mathbb{X}_i^{(l)}(k) | \mathbb{X}_i^{(l)}(k-1), \hat{\mathbf{x}}^{(\neq l)}(k-1)\right)}{q\left(\mathbb{X}_i^{(l)}(k) | \mathbb{X}_i^{(l)}(k-1), \hat{\mathbf{x}}^{(\neq l)}(k-1), \mathbf{z}(k)\right)}, \quad (31)$$

where  $\hat{\mathbf{x}}^{(\neq l)}(\cdot)$  are estimates of the state variables *not* included in the local state vector  $\mathbf{x}^{(l)}(\cdot)$  for subsystem  $S_l$ . Note that Eq. (31) for Subsystem  $S_l$  still requires all observations from the entire network. Clearly, this is impractical. A further approximation is to limit the observation fusion to the neighboring nodes  $\mathcal{G}^{(l)}$ . In other words, observations  $\mathbf{z}(k)$  and estimates  $\hat{\mathbf{x}}^{(\neq l)}(\cdot)$  are replaced with  $\mathbf{z}^{(j)}(k)$  and  $\hat{\mathbf{x}}^{(j)}(\cdot)$  with  $j \in \mathcal{G}^{(l)}$ . This approximation works well due to the localized nature of the observations in the EPG state-space model.

**State Fusion:** The FR/DUPF uses a conservative fusion rule without sending the complete set of particles for shared states. For each shared state  $X_n(k)$ , Subsystem  $S_l$  estimates its mean  $\mu_n^{(l)}(k)$  and covariance  $P_n^{(l)}(k)$  from its weighted particles. The fusion rule [31] is

$$\hat{X}_n^{(\text{fuse})}(k) = \left( \sum_{l \in \mathcal{G}_n} [P_n^{(l)}(k)]^{-1} \right)^{-1} \left( \sum_{l \in \mathcal{G}_n} [P_n^{(l)}(k)]^{-1} \mu_n^{(l)}(k) \right), \quad (32)$$

with covariance  $\hat{P}_n^{(\text{fuse})}(k) = \sum_{l \in \mathcal{G}_n} [P_n^{(l)}(k)]^{-1}$ . The summation terms in Eq. (32) are computed using average consensus [22] within state neighborhoods  $\mathcal{G}_n$ . Once the state fusion process for state  $X_n(k)$  is complete,  $S_l \in \mathcal{G}_n$  generates its local particles for  $X_n$  from the Gaussian distribution  $\mathcal{N}(\hat{X}_n^{(\text{fuse})}(k), \hat{P}_n^{(\text{fuse})}(k))$ .

**Computing Forcing Terms:** The final step in the FR/DUPF is to compute  $\mathbf{d}^{(l)}(k)$  and  $\hat{\mathbf{x}}^{(\neq l)}(k)$  for the next iteration  $(k+1)$ . At this stage, all subsystems have consistent estimates for their shared states. Subsystem  $S_l$  requests the required forcing term  $\mathbf{d}^{(l)}(k)$  from its neighbors  $S_j \in \mathcal{G}^{(l)}$ . This complete iteration  $k$  of the FR/DUPF.

**Computational Complexity** Following [37], the computational complexity of the particle filter with  $n_x$  state variables and  $N_s$  vector particles of dimensions of  $(n_x \times 1)$  is roughly of  $O(n_x^2 N_s)$  flops. Partitioning the system into  $n_{\text{sub}}$  subsystems, the number of state variables per subsystem is roughly  $n_x/n_{\text{sub}}$ . If  $N_s$  vector particles are maintained for each reduced state at each subsystem and assuming no shared state variables between subsystems, the complexity of the FR/DUPF is  $n_{\text{sub}} \times O((n_x/n_{\text{sub}})^2 N_s) \approx O(n_x^2 N_s/n_{\text{sub}})$  leading to a computational saving of a factor of  $n_{\text{sub}}$  in favor of FR/DUPF.

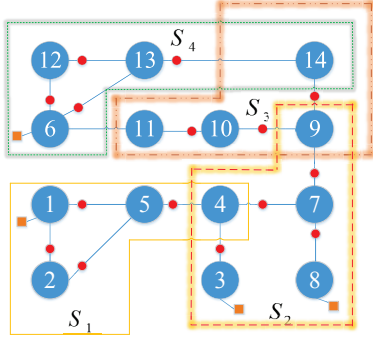


**Fig. 2.** IEEE 14-bus test system spatially decomposed into 4 coupled subsystems used in our simulations. Nodes  $\{1, 2, 3, 6, 8\}$  correspond to the generator nodes for which  $\{V_i, \theta_i, \omega_i\}$  form the states. The remaining 9 nodes are loads for which  $\{V_i, \theta_i\}$  form the states, leading to a total of 32 states.

#### 4. MONTE CARLO SIMULATIONS

In our comparison, three different schemes: (i) The centralized particle filter; (ii) The FR/DUPF, and; (iii) The distributed reduced-order implementation with completely decoupled subsystems (obtained by dropping shared states from state vectors of subsystems where they are not directly observed), are applied to the IEEE 14-bus test system (Fig. 2), which represents a portion of the EPG in the Midwestern USA. Each bus is represented by a number from 1 to 14, which along with its interconnections and external devices forms a node. All generators are assumed similar with their inertia constant  $J$  set to 1.26, damping coefficient  $D = 2$ , time constant  $T_{do} = 0.25$ ,  $X_d - X'_d = 1.05 - 0.1850 = 0.865$ , and time step  $\Delta T$  set to 0.01s.

The centralized implementation assumes all observations are available at the fusion centre. For each state variable, 500 particles represent its posterior density. There are 32 state variables leading to a total of 16,000 particles used in the centralized filter. Initial conditions include: (i)  $P(\mathbf{x}(0))$  assumed to be Gaussian with known error covariance and mean vector, and; (ii) Gaussian state and observation noises,  $\{\zeta(k) \sim \mathcal{N}(\mathbf{x}; \boldsymbol{\mu}_s, \mathbf{R})$  where  $\boldsymbol{\mu}_s$  is the state noise mean vector and  $\mathbf{R}$  its covariance matrix and  $\xi(k) \sim \mathcal{N}(\mathbf{x}; \boldsymbol{\mu}_o, \mathbf{Q})$  where  $\boldsymbol{\mu}_o$  is the observation mean vector with  $\mathbf{Q}$  the observation covariance matrix. Both  $\mathbf{Q}$  and  $\mathbf{R}$  are diagonal, i.e.,  $\mathbf{Q} = \sigma_Q^2 \mathbf{I}$  and  $\mathbf{R} = \sigma_R^2 \mathbf{I}$  with  $\sigma_Q = 0.1$  and  $\sigma_R = 1$ . Before conducting our study, the discretized model is spun-up from rest and integrated forward in time. Data is generated by running initial perturbations based on Eqs. (2)-(6). The resulting fields provide the starting point for the centralized implementation. Observations are based on (8)-(11). A subset of power flows and injections (19 in total with 15 power flow measurements shown as red circles and 4 power injection measurements shown as orange rectangles in Fig. 2) form the observation vector. The setup is similar to [12] used for static state estimation. Noise samples drawn from known distributions are added to measurements to account for observation uncertainties.

As shown in Fig. 2, the FR/DUPF decomposes the IEEE 14-bus test system into 4 subsystems  $\{S_1, S_2, S_3, S_4\}$ . The observations are the same as for the centralized case except they are parsed to associate the resulting subsets  $\mathbf{z}^{(l)}(k)$  with the relevant subsystems  $S_l$ , ( $1 \leq l \leq 4$ ). In total, six states included in the local vectors are shared between the subsystems in the example FR/DUPF simulation. To maintain the same number of particles as were used in the centralized filter, the FR/DUPF associates  $(500 \times 32)/38 = 421$  particles to each of the local state variables. Initialization for the

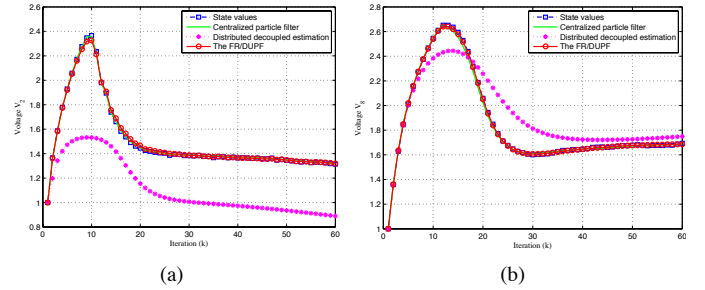


**Fig. 3.** Comparison of the estimated voltage magnitudes from the centralized particle filter, FR/DUPF, and distributed decoupled implementation with the true voltage values for: (a)  $V_2(k)$  at Subsystem  $S_1$ , and (b)  $V_8(k)$  at  $S_3$ .

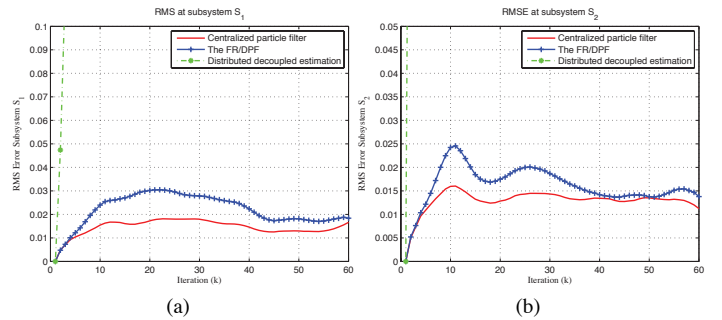


**Fig. 4.** RMS errors for state estimates of  $V_2(k)$  and  $V_8(k)$  plotted in Fig. 3. The RMS errors for the FR/DUPF and centralized particle filter are small and close as compared to their distributed decoupled implementation.

FR/DUPF is the same as performed for the centralized case.

Fig. 3 shows the time evolution of the estimates for two randomly selected states (voltage magnitudes at nodes 2 and 8). As observed from Fig. 3, the estimates from the FR/DUPF and its centralized counterpart follow closely the true states' values implying that the particle filter is a good solution to the state estimation problem in EPGs. Importantly, the FR/DUPF is a good approximation to the centralized filter. The results obtained from the distributed estimator with decoupled subsystems show large errors. Figs. 4 compares the root mean square (RMS) differences between the estimated and true values obtained using the FR/DUPF, decoupled, and centralized filters based on a Monte Carlo simulation averaging RMS errors over 100 runs. The results corroborate our earlier inference that the FR/DUPF is a near-optimal solution to the centralized particle filter.

#### 5. SUMMARY

The paper addressed the problem of nonlinear data fusion in large scale, geographically distributed dynamical EPGs observed sparsely by a network of spatially dispersed nodes. The large dimension of the state vector precludes the centralized filter. The proposed FR/DUPF partitions the EPG into several localized but coupled subsystems distributing the unscented particle filter over the subsystems. Observation and state fusion steps between neighboring subsystems maintain consistency across the EPG. The FR/DUPF provides computational savings of the order of the number of subsystems. In our IEEE 14-bus test system based Monte Carlo simulations, the FR/DUPF and centralized filter are virtually indistinguishable.

## 6. REFERENCES

- [1] Yih-Fang Huang, S. Werner, J. Huang; N. Kashyap, V. Gupta, "State Estimation in Electric Power Grids: Meeting New Challenges Presented by the Requirements of the Future Grid," *IEEE Signal Processing Magazine*, vol. 29, no. 5, pp. 33-43, 2012.
- [2] M.B. Do Coutto Filho and J.C.S. De Souza, "Forecasting-Aided State Estimation Part I: Panorama," *IEEE Transactions on Power Systems*, vol. 24, no. 4, pp. 1667-1677, 2009.
- [3] M.B. Do Coutto Filho and J.C.S. De Souza, R.S. Freund, "Forecasting-Aided State Estimation Part II: Implementation," *IEEE Transactions on Power Systems*, vol. 24, no. 4, pp. 1678-1685, 2009.
- [4] A. S. Debs and R. E. Larson, "A dynamic estimator for tracking the state of a power system," *IEEE Trans. Power App. Syst.*, vol. 89, no. 7, pp. 1670-1678, 1970.
- [5] A. M. Leite da Silva, M. B. Do Coutto Filho, and J. F. de Queiroz, "State forecasting in electric power systems," *Inst. Elect. Eng. Proc., Gener., Trans. Distrib.*, vol. 130, no. 5, pp. 237-244, 1983.
- [6] E. Ghahremani and I. Kamwa, "Dynamic State Estimation in Power System by Applying the Extended Kalman Filter With Unknown Inputs to Phasor Measurements," *IEEE Transactions on Power Systems*, vol. 26, no. 4, pp. 2556-2566, 2011.
- [7] S. Wang, W. Gao, A.P.S. Meliopoulos, "An Alternative Method for Power System Dynamic State Estimation Based on Unscented Transform," *IEEE Transactions on Power Systems*, vol. 27, no. 2, pp. 942-950, May 2012.
- [8] G. Valverde, V. Terzija, "Unscented kalman filter for power system dynamic state estimation," *IET Generation, Transmission & Distribution*, vol. 5, no. 1, pp. 29-37, Jan. 2011.
- [9] E. Ghahremani, I. Kamwa, "Online State Estimation of a Synchronous Generator Using Unscented Kalman Filter From Phasor Measurements Units," *IEEE Transactions on Energy Conversion*, vol. 26, no. 4, pp. 1099-1108, Dec. 2011.
- [10] M.D. Ilicc, Le Xie, U.A. Khan, J.M.F. Moura, "Modeling of Future CyberPhysical Energy Systems for Distributed Sensing and Control," *IEEE Transactions on Systems, Man and Cybernetics, Part A: Systems and Humans*, vol. 40, no. 4, pp. 825-838, 2010.
- [11] Le Xie, Dae-Hyun Choi, S. Kar, H.V. Poor, "Fully Distributed State Estimation for Wide-Area Monitoring Systems," *IEEE Transactions on Smart Grid*, vol. 3, no. 3, pp. 1154-1169, 2012.
- [12] G.N. Korres, "A Distributed Multiarea State Estimation," *IEEE Transactions on Power Systems*, vol. 26, no. 1, pp. 73-84, 2011.
- [13] V. Kekatos and G.B. Giannakis, "Distributed Robust Power System State Estimation," *IEEE Transactions on Power Systems*, vol. 28, no. 2, pp. 1617-1626, 2013.
- [14] G.G. Rigatos and P. Siano, "Distributed state estimation for condition monitoring of nonlinear electric power systems," *IEEE Inter. Symp. on Industrial Electronics*, pp.1703-1708, 2011.
- [15] M. Dehghani, S. Nikravesh, "State-Space Model Parameter Identification in Large-Scale Power Systems," *IEEE Transactions on Power Systems*, vol. 23, no. 3, pp. 1449-1457, 2008.
- [16] H. Mingguo, L. Chen-Ching and M. Gibescu, "Complete controllability of an N-bus dynamic power system model," *IEEE Transactions on Circuits and Systems I: Fundamental Theory and Applications*, vol. 46, no. 6, pp. 700-713, 1999.
- [17] M. Dehghani and S. K. Y. Nikravesh, "Nonlinear state space model identification of synchronous generators," *Elect. Power Syst. Res.*, vol. 78, no. 5, pp. 926-940, 2008.
- [18] N. Gordon, M. Sanjeev, S. Maskell, and T. Clapp, "A tutorial on particle filters for online nonlinear/non-gaussian bayesian tracking," *IEEE Trans. on Sig. Proc.*, vol. 50, pp. 174-187, 2002.
- [19] R. Van der Merwe, A. Doucet, N. de Freitas and E. Wan, "The unscented particle filter," Tech. Rep. CUED/F-INFENG/TR 380, Cambridge University, 2000.
- [20] M. Briers, A. Doucet and S. S. Singh, "Sequential auxiliary particle belief propagation", *Int. Conf. on Inf. Fusion*, pp. 705-711, 2005.
- [21] M.F. Bugallo, Ting Lu and P.M. Djuric, "Target Tracking by Multiple Particle Filtering," *Aerospace Conference*, pp.1-7, 2007.
- [22] A. Mohammadi and A.Asif, "Distributed Particle Filter Implementation with Intermittent/Irregular Consensus Convergence," *IEEE Trans. on Sig. Proc.*, vol. 61, no. 10, pp. 2572-2587, May15, 2013.
- [23] A. Mohammadi and A.Asif, "Full Order Nonlinear Distributed Estimation in Intermittently Connected Networks", in *IEEE Inter. Conf. on Acoustics, Speech and Signal Proc. (ICASSP)*, 2013.
- [24] A. Mohammadi and A. Asif, "A Constraint Sufficient Stas based Distributed Particle Filter for Bearing Only Tracking", *IEEE International Conference on Communication (ICC)*, pp. 3670-3675, 2012.
- [25] O. Hlinka, F. Hlawatsch, and P.M. Djuric, "Distributed Particle Filtering in Agent Networks: A Survey, Classification, and Comparison," *IEEE Signal Processing Magazine*, vol. 30, no. 1, pp. 61-81, Jan. 2013.
- [26] S. Farahmand, S. I. Roumeliotis, and G. B. Giannakis, "Set-membership constrained particle filter: Distributed adaptation for sensor networks," *IEEE Trans. on Signal Processing*, vol. 59, no. 9, pp. 4122-4138, Sept. 2011.
- [27] D. Ustebay, M. Coates, and M. Rabbat, "Distributed auxiliary particle filters using selective gossip," In *IEEE Inter. Conf. on Acoustics, Speech and Signal Proc. (ICASSP)*, pp. 3296-3299, 2011.
- [28] A. Mohammadi and A. Asif, "Theoretical Performance Bounds for Reduced-order Linear and Nonlinear Distributed Estimation," *IEEE Global Communications Conference (GLOBECOM)*, pp. 3929-3935, 2012.
- [29] A. Mohammadi and A. Asif, "Distributed State Estimation for Large-scale Nonlinear Systems: A Reduced Order Particle Filter Implementation," *IEEE Statistical Sig. Proc. (SSP)*, pp. 249-252, 2012.
- [30] A. Mohammadi and A. Asif, "Distributed particle filtering for large scale dynamical systems," In *IEEE 13th Inter. Multitopic Conference*, pp.1-5, 2009.
- [31] U.A. Khan and J.M.F. Moura, "Distributing the Kalman filter for large-scale systems," *IEEE Trans. on Signal Processing*, vol. 56, no.10, pp. 4919-4935, 2008.
- [32] T.M. Berg and H.F. Durrant-Whyte, "Model distribution in decentralized multi-sensor data fusion," *American Cont. Con.*, pp. 2292-2293, 1991.
- [33] F. Daum and J. Huan, "Curse of Dimensionality and Particle Filters," *IEEE Conference on Aerospace*, pp. 4.1979-4.1993, 2003.
- [34] T. Bengtsson, P. Bickel and B. Li, "Curse of dimensionality revisited: Collapse of the particle filter in very large scale systems", in *IMS Lecture Notes - Monograph Series in Probability and Statistics: Essays in Honor of David A. Freedman*, Institute of Mathematical Sciences, pp. 316-334, 2008
- [35] G. Andersson, "Modelling and Analysis of Electric Power Systems", *ETH Zurich*, 2009.
- [36] D.A. Forsyth and J. Ponce. "Computer Vision : A Modern Approach", *Prentice Hall*, 2003.
- [37] R. Karlsson, T. Schon, and F. Gustafsson, "Complexity Analysis of the Marginalized Particle Filter," *IEEE Trans. Signal Processing*, vol. 53, no. 11, pp. 4408-4411, 2005.
- [38] S. K. M. Kods and C. A. Canizares, "Modeling and Simulation of IEEE 14-bus System with FACTS Controllers," *Tech. Rep., Univ. of Waterloo*, Mar. 2003.
- [39] A. Mohammadi and A. Asif, "Posterior Cramer-Rao Bounds for Full and Reduced-order Distributed Bayesian Estimation," accepted in *IEEE Transactions on Aerospace and Electronic Systems*, 2013. manuscript of 38 pages. in press.